Fast Ring-Opening Metathesis Polymerization of Tricyclic Oxanorbornene Derivatives

Zhenghao Dong, Peng Liu, Aurelien Crochet, Andreas F. M. Kilbinger*

* Department of Chemistry, University of Fribourg, Chemin du Museé 9, CH-1700 Fribourg, Switzerland, andreas.kilbinger@unifr.ch

ABSTRACT

A new type of tricyclic oxanorbornene monomer was developed for living ring-opening metathesis polymerization (ROMP). A methyl group located at the endo-position of the oxanorbornene bicycle resulted in polymerization kinetics orders of magnitude slower than the corresponding hydrogen-substituted monomers because of steric effects. Both monomers showed well-controlled molecular weights and excellent dispersities with Grubbs' third-generation catalyst. The slower endo-methyl substituted monomers could even be polymerized in a well-controlled manner using Grubbs' second-generation catalyst. Investigations of random copolymers demonstrated that the steric hindrance only affects the rate of propagation rather than the rate of initiation. Block copolymers between the fast and slow monomers could be prepared with good molecular weight and dispersity control.

INTRODUCTION

Ring opening metathesis polymerization (ROMP), as an efficient and reliable technique for synthesizing linear polymers, has been widely used in material science, academic research and industrial applications.[1-8] In ROMP, norbornene and its derivatives are most commonly used due to their high ring strain and easy incorporation of substituents.[9] Oxanorbornenes are structurally similar to norbornenes, however, they are typically prepared from furan derivatives, such as furfural, a renewable resource obtained from agricultural waste.[10,11] Oxanorbornenes, therefore, have a unique advantage over traditional norbornene derivatives in terms of ecologic friendliness while being similarly reactive.[12,13]

Typically, oxanorbornenes are synthesized from furan and an electron deficient olefin via the Diels-Alder (D-A) reaction.[14-26] Michael North's group explored derivatives of oxanorbornene **1** as novel reactive monomers for the synthesis of polymers via ROMP with Grubbs' second-generation catalyst (G-II, **2**).[15-17] G-II (**2**) possesses an exceptionally high activity in olefin metathesis and is often employed for cross and ring-closing metatheses.[27-29] Nevertheless, it typically yields polymers with uncontrolled molecular weights and large dispersities owing to its slow initiation and high propagation rates (low ki/kp; ki = the rate constant for initiation, kp = the rate constant for propagation)[30,31] and competing chain-transfer reactions.[32-34] However, the polymerization of monomers was typically very slow (up to 72 h) causing difficulties to form large block copolymers which limited their applications in ROMP. Then, structurally similar *N*-substituted lactams derivatives of oxanorbornene **4** possessing an exo-orientated carboxylic acid were found to display well-controlled and extremely rapid polymerizations in the presence of Grubbs 3rd generation catalyst (G-III, **5**). [18,19] Here, we describe the synthesis of several tricyclic monomers suitable for

living ROMP based on biomass derived furfuryl amine. The monomers can be readily functionalized and, despite their bridgehead substitution, often polymerized rapidly.

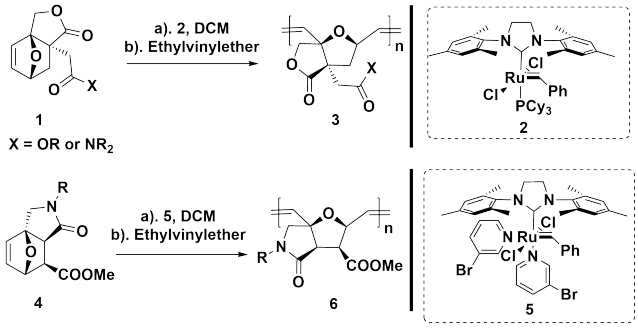

Scheme 1. Previous work on the synthesis of bio-based ROMP polymers from oxanorbornenes

RESULTS AND DISCUSSION

To avoid a sterically demanding substituent (CH_2COX) in the endo-position of the oxanorbornene ring, we designed a secondary amine derivative of furan (**7**) as the starting material to carry out an amidation followed by a Diels-Alder (D-A) reaction with (meth)acryloyl chloride (**8, 9**). In this way we obtained a tricyclic *N*-substituted lactam derivative of oxanorbornene (**10**, **11**) (Scheme 2). Only the *exo*-derivatives of the fused lactam ring were formed in monomers **10** and **11** presumably due to a lower ring strain compared to the hypothetical lactam ring formed between the bridgehead and the *endo*-position.

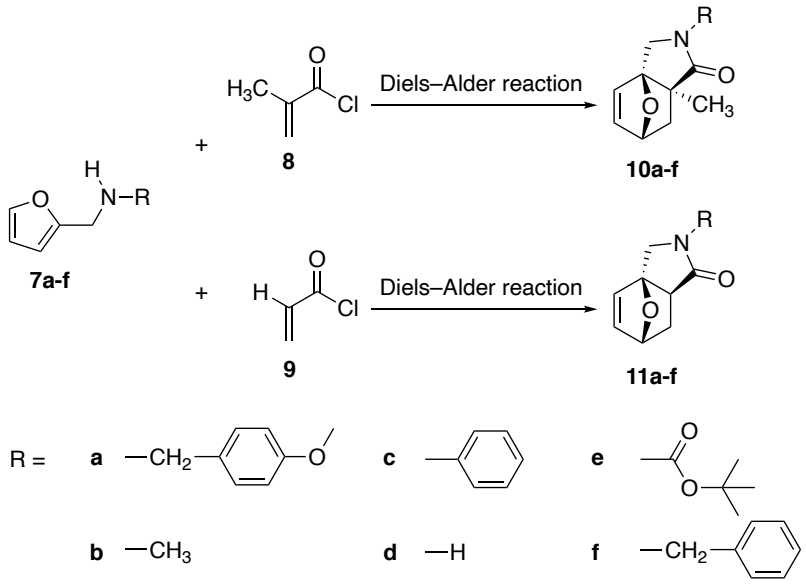

Scheme 2. Synthesis of bridgehead-substituted oxanorbornene monomers **10a-f** and **11a-f**.

Monomers **10** and **11** are identical except for an endo-methyl group in the 6-position of the oxanorbornene bicycle. We attempted a polymerization initiated with G-II (2 mol%) in dichloromethane (DCM) with monomer **10a** and **11a** respectively. As we expected, **11a** formed a gel immediately upon exposure to G-II indicating the formation of a high molecular weight polymer and loss of molecular weight control. Monomer **10a** on the other hand formed a polymer within 10 hours with a molecular weight that was just little higher than the one aimed for ($M_{n(obtained)}$ = 1.91×10^4 vs. $M_{n(target)}$ = 1.43×10^4) but exhibiting a very good dispersity (Đ = 1.13) based on chloroform gel permeation chromatography (GPC). Subsequently, following the same protocol, we successfully obtained the homopolymers **poly-10a** and **poly-10b**, which had controlled molecular weights (too high by ca. 30-70%) and narrow dispersities (Đ ≤ 1.18; table 1, entry 1 - 2) at varying monomer to initiator ratios.

Next, Grubbs' third-generation catalyst (G-III, **5**) was investigated as initiator in ROMP with monomers **10** due to its rapid rate of initiation (high ki/kp).[35] As expected, the polymerizations of

monomers (**10a, 10b, 10f**) exhibited better molecular weight control and better dispersities (Đ ≤ 1.10, Table 1, 3 - 4, 6) when varying the monomer to initiator ratios compared to those shown for G-II (Table 1). Similar result was obtained for the polymerization of monomer **10c** (Table 1, entry 5) for monomer to initiator ratios smaller than 60 :1 (for ratios greater than 50:1, the polymer starts to precipitate from chloroform solution and it was difficult to detect the signal peak in the chloroform GPC). Although the homopolymerizations of monomers **10d** and **10e** occurred successfully in DCM with nearly full conversion, the polymers precipitated during the polymerization and after work-up the dried polymers obtained were insoluble in all solvents (chloroform, THF, DMF) tested.

Table 1. Molecular weight data for the homopolymerization of monomers **10** at varying monomer (**10a-10c, 10f**) to initiator (G-II**,** G-III) molar ratios. [a]

entry	Monomer(-R)	catalyst	ratio[b]	$M_{n.calc.}$ (kDa)[c]	$M_{n.obs}$(kDa)[d]	Đ[d]
1	10a(-PMB)	G-II	25	7.1	11.8	1.10
			50	14.3	19.1	1.13
			75	21.4	29.9	1.10
			100	28.5	37.3	1.10
2	10b(-Me)	G-II	50	9.0	15.3	1.15
			75	13.4	21.7	1.18
			100	17.9	28.0	1.13
3	10a(-PMB)	G-III	20	5.7	6.0	1.07
			30	8.6	9.6	1.06
			40	11.4	11.0	1.08
			50	14.3	16.2	1.04
			100	28.5	30.8	1.03
4	10b(-Me)	G-III	30	5.4	5.5	1.09
			40	7.2	9.7	1.06
			50	9.0	11.3	1.07
			100	17.9	21.0	1.04
5	10c(-Ph)	G-III	30	7.2	7.0	1.07
			40	9.6	11.6	1.05
			50	12.1	13.0	1.06
			60	14.5	16.0	1.04
6	10f(-Bn)	G-III	30	6.4	8.2	1.06
			40	10.2	9.2	1.10
			50	12.8	16.0	1.04
			100	25.5	29.8	1.03

[a] All reactions were carried out at room temperature in dichloromethane and all reactions had gone to completion overnight. [b] monomer/catalyst. [c] calculated from the theoretical degree of polymerization. [d] determined by GPC (chloroform).

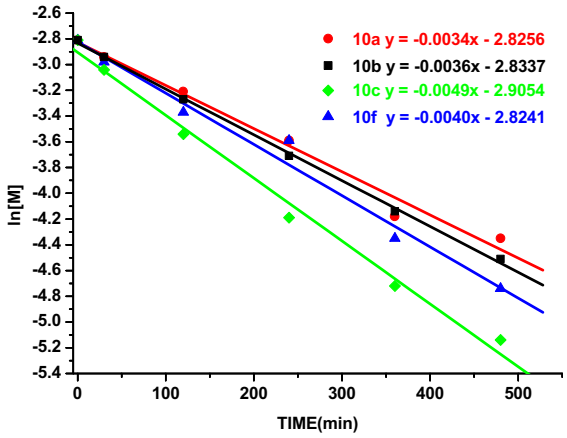

Figure 1. Propagation kinetics of monomers **10a-c**, **10f** (0.06 mmol) using initiator **5** (0.002 mmol) in 1 mL DCM-d_2.

However, regardless of whether G-II or G-III was used as the initiator, all polymers obtained showed a linear relationship between molecular weight and monomer/catalyst ratio (supporting information Figure S79). Overall, G-III can clearly improve the molecular weight control and dispersity for monomers **10**, but it does not significantly shorten the reaction time.

In addition, we attempted to extract kinetic data from the signal intensities obtained by ^{1}H NMR spectroscopy of monomers **10a-c**, **10f**. 1,3,5-Trimethoxybenzene was used as internal standard (ppm = 5.95 - 6.00) to measure and calculate the consumption of monomers **10** (ppm = 6.20 - 6.40) with G-III. The data obtained was found to fit first order kinetics with kinetic constants k ranging from 5.7 - 8.2 x 10^{-5} s^{-1} at 298 K (Figure 1, supporting information Table and Figure S1-S4), which represented an increase by an order of magnitude compared to monomer **1** (Scheme 1)[16,17]. Next, the same protocol was employed to explore the polymerization kinetics of monomer **10f** with initiator G-II (supporting information Table and Figure S5). As shown in Figure 2, G-II showed its lower initiation efficiency in ROMP (< 60 min) compared with G-III. However, we observed that the character of slow propagation made the conversion of monomer **10f** with G-II fit to zero

order kinetics (> 60 min， Figure 2). Meanwhile we continued to observe the signal peak belonging to the non-initiated benzylidene complex of G-II at 19.1 ppm by ^{1}H NMR spectroscopy despite the monomer having been consumed completely (supporting information, Figure S5). The fraction of unreacted G-II benzylidene complex also explained why the molecular weights obtained were much higher than calculated. We, therefore, concluded that the low propagation rate of the monomer could partly compensate the poor initiation characteristics of G-II.

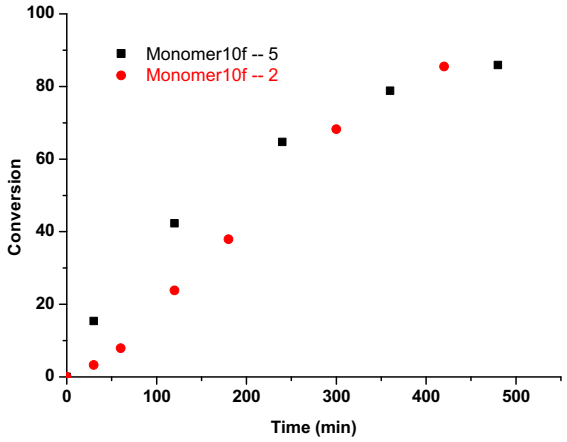

Figure 2. Polymerization of monomer **10f** with catalysts G-II and G-III. Monomer conversion is plotted vs. reaction time. The data originated from Table S4 - S5 and Figure S4 - S5 in the supporting information.

Compared with the slow monomers **10**, monomers **11a-11c** polymerized to completion within 5 minutes using initiator G-III (Figure 3a) which was too fast to capture kinetic data by ^{1}H-NMR spectroscopy.

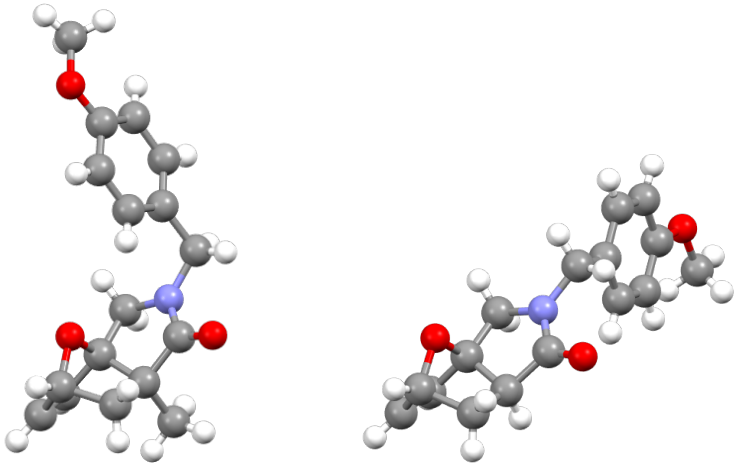

Scheme 3. X-ray single crystal structures of monomers **10a** (left) and **11a** (right).

Table 2. Molecular weight data for the homo polymerization of monomers **11** at varying molar ratios with respect to catalyst. [a]

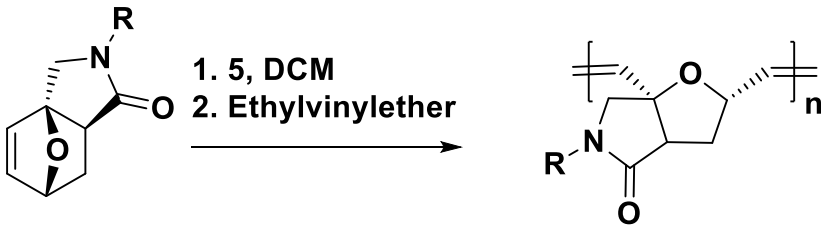

entry	Monomer(-R)	catalyst	Ratio	$M_{n.calc.}$ (KDa)[b]	$M_{n.obs}$(KDa)[c]	Đ[c]
1	11a(-PMB)	G-III	25	6.8	6.2	1.08
			50	13.6	13.5	1.04
			75	20.3	21.0	1.06
			100	27.1	31.1	1.06
2	11b(-Me)	G-III	25	4.1	2.9	1.08
			50	8.3	5.9	1.11
			75	12.4	8.5	1.07
			100	16.5	10.7	1.11
3	11c(-Ph)	G-III	25	5.7	6.1	1.07
			50	11.4	12.3	1.04
			75	17.0	16.7	1.05
			100	22.7	21.3	1.05

[a] All reactions were carried out at room temperature in dichloromethane and all the reactions had gone to completion within 30 min. [b] calculated from the theoretical degree of polymerization. [c] determined by GPC (chloroform).

The polymers obtained showed controlled molecular weights, narrow dispersities (Table 2) and a linear relationship between molecular weight and monomer/ catalyst ratio (supporting information Figure S80). Moreover, the solubility of **poly-11c** in chloroform was significantly improved compared to **poly-10c**. The only difference between the two monomers is the methyl group located at the endo-position, which is clearly the reason hindering the propagation in ROMP. In order to confirm the steric effect of the methyl group in ROMP, two single crystals (**10a**, **11a**; Scheme 3) were grown (chloroform and hexane, see supporting information) and analyzed by single crystal x-ray diffraction. It appears unlikely that either the *exo*-lactam ring (**10a**,**11a**) or the *endo*-methyl group (**10a**) affect the coordination of the ruthenium carbene complex to the *exo*-face of the oxanorbornene double bond. A hindered propagation after ring-opening of the oxanorbornene bicycle is, therefore, a more likely scenario in our opinion.

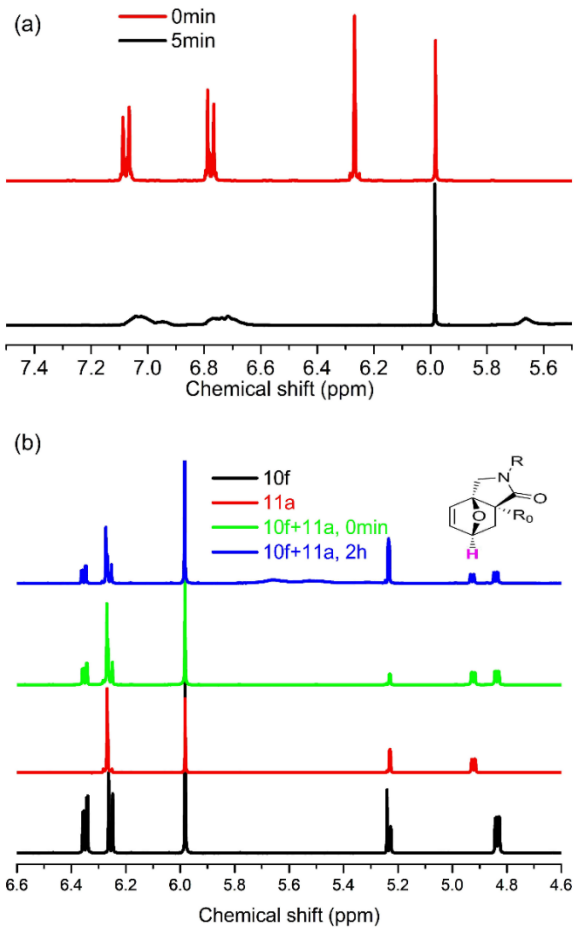

Figure 3. ^{1}H-NMR spectra showing the region of the double bond signals in monomers **11a** and **10f**. (a) ^{1}H NMR spectra for monomer **11a** (red, top). The monomer was consumed completely within 5 minutes after G-III was added (black spectrum, bottom). (b) ^{1}H NMR spectra recorded of the copolymerization of monomers **11a** and **10f** with G-III, blue). The pure monomers **10f** (black) and **11a** (red) as well as the mixture of both (green) before addition of G-III is shown. The polymerization rate is drastically reduced by the addition of **10f** to **11a** (blue spectrum after 2h of polymerization time).

To prove this hypothesis, we attempted to introduce 1,5-cyclooctadiene (COD), which is sterically unhindered, to the polymerization of **10f**. We observed that with increasing amounts of COD, monomer **10f** could complete full monomer conversion in shorter time (Figure 4), e.g., the polymerization completed in 2 hours instead of 10 hours when 4 equiv of COD were added. This supported our hypothesis that the ring-opening reaction of **10f** was indeed fast and that the resulting ruthenium carbene complex was sterically very demanding. This sterically demanding carbene complex is slow to react with another larger monomer **10f** but reacts quickly with the sterically less demanding COD. The ring-opened COD on the other hand represent a ruthenium-carbene complex of very low steric demand and can, therefore, immediately react with **10f**, which has a higher ring strain than COD. In this manner addition of COD results in an increased consumption of **10f**.

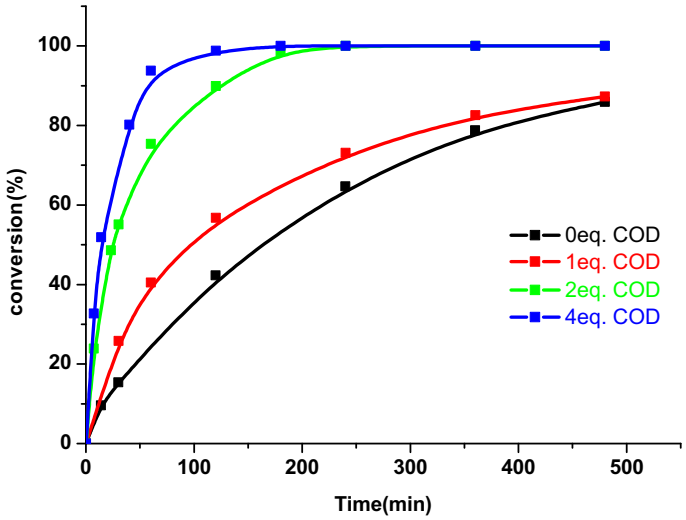

Figure 4. Following the copolymerization of monomer **10f** and 0 - 4 equivalents of **COD** over time. The data originated from Table S6 and Figure S4, S84 - S86 in the supporting information.

We noticed that even after a polymerization time of 2 hours, monomer **11a** (δ = 4.8 - 5.0 ppm) could still be observed in the mixture and that it was consumed at the same rate as monomer **10f**.

Furthermore, a mixture of equal amounts of fast monomer **11a** (15 equiv) and slow monomer **10f** (15 equiv) were investigated in a copolymerization with G-III followed by ^{1}H-NMR spectroscopy (Figure 3b). This was totally contradictory to the block-like copolymer synthesized in one step using a mixture of fast and slow monomers reported by us previously.[36] From this observation we conclude that our initial hypothesis was correct and that the cross-propagations of monomers **11a** and **10f** must be virtually identical. In other words, both **10f** and **11a** are initiated equally quickly and hence statistically and, therefore, the retarded propagation of **10f** can slow down the entire copolymerization.

Subsequently, we examined the potential of block copolymerization of these two monomers. We set up two polymerizations using **10f** (50:1 monomer/initiator **5**) as the first polymer block. After 10 hours, either 10 equivalents of monomer **10a** or monomer **11a** were added and the polymerizations continued for a further 10 hours or 30 minutes, respectively. The resulting two block copolymers both showed low dispersities (Table 3, entry 1 and 2) when analyzed by chloroform GPC. We then selected two monomers for the second block of diblock copolymers who's respective homopolymers were insoluble in many solvents (**10d** and **10e**, see above). Block copolymer poly(**10f**-*b*-**10e**) showed good molecular weight and dispersity control (Đ = 1.03, Table 3, entry 3) while the block copolymer poly**(10f**-*b*-**10d)** showed a molecular weight lower than targeted (16.3 vs 27.2 kDa) but with good dispersitiy (Đ = 1.26 (Table 3, entry 4) based on chloroform GPC. After deprotection of the BOC protecting group in poly(**10f**-*b*-**10e**) (Table 3, entry 5), the observed (GPC) molecular weight was also much lower than calculated and the GPC retention time was almost identical to that of poly**(10f**-*b*-**10d)** (Figure 5a). We speculate that intramolecular H-bonds of the amide containing polymer block (**10d**) are responsible for a

reduction of the hydrodynamic radius and hence apparent lower molecular weight in GPC measurements.

Table 3. Molecular weight data for the block copolymerization at varying monomer to catalyst molar ratios.[a]

Entry	monomer 1	monomer 2	catalyst	ratio	$M_{n.calc.}$ (KDa)[h]	$M_{n.obs}$ (KDa)[i]	Đ[i]
1	10f[b]	10a[e]	G-III	50/10/1	15.6	19.0	1.04
2	10f[b]	11a[f]	G-III	50/10/1	15.5	14.9	1.04
3	10f[b]	10e[e]	G-III	100/10/1	28.2	30.5	1.03
4	10f[b]	10d[e]	G-III	100/10/1	27.2	16.3	1.26
5	10f[b]	10d[e,g]	G-III	100/10/1	27.2	18.9	1.16
6	10f[b]	11a[f]	G-III	50/50/1	26.3	33.0	***1.03***
7	11f[c]	10a[e]	G-III	50/50/1	26.3	23.8	1.14
8	11f[d]	10a[e]	G-III	50/50/1	26.3	22.0	1.14
9	11f[d]	11a[f]	G-III	50/50/1	25.6	22.9	1.14

[a] Unless indicated all reactions were carried out at room temperature in dichloromethane. [b] 10 hours between addition of monomers. [c] 30 minutes between addition of monomers. [d] 10 minutes between addition of monomers. [e] 10 hours reaction time. [f] 30 minutes reaction time. [g] BOC-deprotected form of poly(**10e**) block. [h] M_n was calculated from the theoretical degree of polymerization. [i] Determined by GPC (chloroform); dispersities shown in bold italics do not represent the entire distribution but only the highest molecular weight peak in a bimodal distribution

Next, we attempted to prepare a diblock copolymer from equal amounts of monomers **10f** and **11a** initiated with G-III (50/50/1). Unfortunately, the polymer obtained showed a bimodal distribution in GPC (chloroform). We believe that propagating poly(**10f**) based on a slower, sterically hindered monomer, is a poor macroinitiator. In combination with the faster monomer **11a** at higher concentration (Table 3 entry 6) peak broadening and a bimodal distribution can be expected due to incomplete macro-initiation. We, therefore, continued to investigate diblock copolymers in which the first polymer block was always based on fast monomer **11f**.

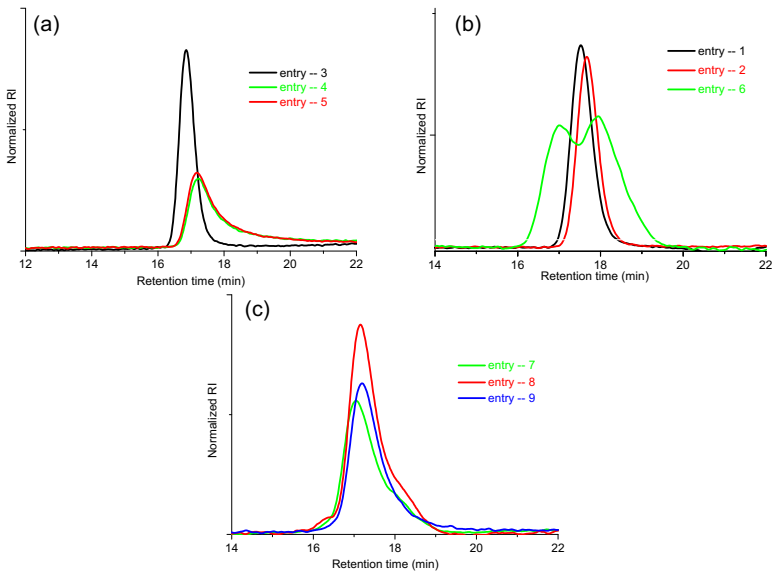

Figure 5. Normalized GPC refractive index traces with block polymer.

We next polymerized monomer **11f** as the first polymer block, which was consumed completely within 5 minutes (Figure 3a). After 30 minutes, 50 equivalent of either monomers **10a** or **11a** were added in three different experiments (Table 3, entries 7, 8, 9; Figure 5 c entries 7, 8, 9). In the first two experiments, monomer **10a** was added after either 30 min or 10 min to the propagating poly(**11f**). Almost identical GPC (chloroform) traces were observed for both diblock copolymers (Figure 5 - c, entries 7, 8). However, when monomer **11a** was added to propagating poly(**11f**) a diblock copolymer was obtained with a noticeable shoulder towards lower molecular weights (chloroform GPC). As both monomers **11a** and **11f** are sterically unhindered, we believe that subtle kinetic differences might be responsible for the observed shoulder in the GPC elugram. The analogous monomers carrying an endo-methyl group (**10a** and **10f**) were shown to exhibit slight differences in their rate of propagation (Figure 1). Assuming that, in analogy, **11a** propagates

slightly faster than **11f**, this effect could have contributed to the observed shoulder in the GPC trace.

CONCLUSION

In summary, we have successfully developed a new type of biobased tricyclic oxanorbornene derivative for the ring-opening metathesis polymerization. The polymerizations are shown to afford homopolymers with well-controllable molecular weight, excellent dispersities ($Đ \leq 1.10$) and a linear relationship between molecular weight and monomer/ initiator ratio with Grubbs third-generation catalyst (G-III, **5**). Two types of monomers differing in an *endo*-methyl group were prepared via our synthetic pathway. Monomers **11** (without *endo*-methyl group) could be polymerized within minutes, orders of magnitude faster than monomers **10** (carrying the endo-methyl group), which typically needed around 10 hours to polymerize. However, the dramatically reduced rate of propagation of monomers **10** allowed them to be polymerized in a living fashion using Grubbs' 2nd generation initiator (G-II, **2**). Homopolymers with well-controllable molecular weight, good dispersities ($Đ \leq 1.18$) and a linear relationship between molecular weight and monomer/ initiator ratio could be obtained. An NMR study of random copolymer formation between **10f** and cyclooctadiene (COD) as well as **10f** and **11a** suggested that the reactivity of propagating poly (10f) is significantly lower than that of poly (**11a**) while the reactivities of **10f** and **11a** are most likely similar.

Corresponding Author

Andreas F. M. Kilbinger – Department of Chemistry, University of Fribourg, 1700 Fribourg, Switzerland;

orcid.org/0000-0002-2929-7499;

Email: andreas.kilbinger@unifr.ch

ACKNOWLEDGMENTS

The authors would like to thank the State Scholarship Fund of China Scholarship Council (CSC, Scholarship no. 201806180055) and the Fribourg Center for Nanomaterials (Frimat) for funding as well as A. Mandal, I. Mandal and M. Singh for helpful discussions.

References

1. Yamauchi, Y.; Horimoto, N. N.; Yamada,K.; Matsushita, Y. Takeuchi, M. and Ishida, Y. Two-Step Divergent Synthesis of Monodisperse and Ultra-Long Bottlebrush Polymers from an Easily Purifiable ROMP Monomer. *Angew. Chem. Int. Ed.* **2021**, *60*, 1528 – 1534
2. Liu, P.; Ai, C. Olefin Metathesis Reaction in Rubber Chemistry and Industry and Beyond *Ind. Eng. Chem. Res.* **2018**, *57*, 3807 – 3820.
3. Chen, Y.; Abdellatif, M. M.; Nomura, K. Olefin metathesis polymerization: Some recent developments in the precise polymerizations for synthesis of advanced materials (by ROMP, ADMET) *Tetrahedron* **2018**, *74*, 619 – 643.
4. Slugovc, C. in *Industrial applications of olefin metathesis polymerization in Olefin Metathesis* (Ed.: K. Grela), Wiley, Hoboken, **2014**, Chap. 10, pp. 329 – 333.
5. Fishman, J. M.; Kiessling, L. L. Synthesis of Functionalizable and Degradable Polymers by Ring-Opening Metathesis Polymerization *Angew. Chem. Int. Ed.* **2013**, *52*, 5061 – 5064.
6. Madkour, A.; Koch, E.; Lienkamp, A. H. R.; Tew, K. G. N. End-Functionalized ROMP Polymers for Biomedical Applications *Macromolecules*, **2010**, *43*, 4557 – 4561.

7. Hilf, S.; Kilbinger,A. F. M. Functional end groups for polymers prepared using ring-opening metathesis polymerization *Nat. Chem.* **2009**, *1*, 537 – 546.
8. Kolonko, E. M.; Pontrello, J. K.; Mangold, S. L.; Kiessling, L. L. General Synthetic Route to Cell-Permeable Block Copolymers via ROMP *J. Am. Chem. Soc.* **2009**, *131*, 7327 – 7333.
9. S. Sutthasupa, M. Shiotsuki, F. Sanda, *Polym. J.* **2010**, *42*, 905 – 915.
10. Zeitsch, K. J. in *The Chemistry and Technology of Furfural and its Many By-Products*, Vol. 13, Elsevier, Amsterdam, **2000**, p. 376.
11. Lange, J.-P.; Heide, E. V. D.; Buijtenen, J. V.; Price, R. Furfural—A Promising Platform for Lignocellulosic Biofuels *ChemSusChem*. **2012**, *5*, 150 – 166.
12. Liu, P.; Dong, Z.; Kilbinger, A. F. M. Mono-telechelic polymers by catalytic living ring-opening metathesis polymerization with second-generation Hoveyda–Grubbs catalyst *Mater. Chem. Front.* **2020**, *4(9)*, 2791 – 2796.
13. Pehere, A. D.; Xu, S.; Thompson, S. K.; Hillmyer, M. A. and Hoye, T. R. Diels−Alder Reactions of Furans with Itaconic Anhydride: Overcoming Unfavorable Thermodynamics *Org. Lett.* **2016**, *18*, 2584−2587.
14. Liu, P.; Yasir, M.; Kilbinger, A. F. M. Catalytic Living Ring Opening Metathesis Polymerisation: The Importance of Ring Strain in Chain Transfer Agents *Angew. Chem. Int. Ed.* **2019**, *58*, 15278 –15282.
15. Bai, Y.; Bruyn, M. D.; Clark, J. H.; Dodson, J. R.; Farmer, T. J.; Honore, M.; Ingram, I. D. V.; Naguib, M.; Whitwood, A. C.; North, M. Ring opening metathesis polymerisation

of a new bio-derived monomer from itaconic anhydride and furfuryl alcohol *Green Chem*. **2016**, *18*, 3945 – 3948.

16. Bai, Y.; Clark, J. H.; Farmer, T. J.; Ingram, I. D. V.; North, M. Wholly biomass derivable sustainable polymers by ring-opening metathesis polymerisation of monomers obtained from furfuryl alcohol and itaconic anhydride *Polym. Chem*. **2017**, *8,* 3074 – 3081.
17. Lawrenson, S. B.; Hart, S.; Ingram, I. D. V.; North, M.; Parker, R.; Whitwood, A. C. Ring-Opening Metathesis Polymerization of Tertiary Amide Monomers Derived from a Biobased Oxanorbornene *ACS Sustainable Chem. Eng*. **2018**, *6*, 9744 – 9752.
18. Naguib, M.; Schiller, T. L.; Keddie, D. J. Rapid, Regioselective Living Ring-Opening Metathesis Polymerization of Bio-Derivable Asymmetric Tricyclic Oxanorbornenes *Macromol. Rapid Commun*. **2018**, *39,* 1700794.
19. Blanpain, A.; Clark, J. H.; Farmer, T. J.; Guo, Y.; Ingram, I. D. V.; Kendrick, J. E.; Lawrenson, S. B.; North, M.; Rodgers, G.; Whitwood, A. C. Rapid Ring-Opening Metathesis Polymerization of Monomers Obtained from Biomass-Derived Furfuryl Amines and Maleic Anhydride *ChemSusChem*. **2019**, *12*, 2393 – 2401.
20. Lawrenson, S. B.; Pearce, A. K.; Hart, S.; Whitwood, A. C.; O'Reilly, R. K.; North, M. Synthesis of cytotoxic spirocyclic imides from a biomass-derived oxanorbornene *Tetrahedron*. **2021**, *77,* 131754.
21. Fulgheri, T.; Cornwall, P.; Turner, A. R.; Sweeney, J. B. and Gill, D. M. Parallel Kinetic Resolution of Intramolecular Furan Diels-Alder Cycloadducts via Asymmetric Hydroboration *Eur. J. Org. Chem*. **2019**, 7223 – 7227.

22. Mukaiyama, T.; Tsuji, T. and Iwasawa, N. Synthetic Control by Internal Coordination of Metal Salts the Intramolecular Diels-Alder Reactions of N-Furfuryl-N-(2-hydroxyphenyl) Acrylamides *Chemistry letterrs*, **1979,** 697-700.

23. Gschwend, H. W.; Hillman, M. J. and Kisis, B. Intramolecular Diels-Alder reactions. Synthesis of 3a-phenylisoindolines as analgetic templates *J. Org. Chem.* **1976,** 104-110.

24. Parker, K. A. and Adamchuk, M. R. Intramolecular Diels-Alder reactions of the furan diene *Tetrahedron Letters,* **1978,** 19**,** 1689 – 1692.

25. Zaytsev, V. P.; Mertsalov, D. F.; Nadirova, M. A.; Dorovatovskii, P. V.; Khrustalev, V. N.; Sorokina, E. A.; Zubkov, F. I.; Varlamov, A. V. [3+2] Cycloaddition of o-nitrophenyl azide to 3a,6-epoxyisoindoles *Chemistry of Heterocyclic Compounds*. **2017**, *53(11)*, 1199 – 1206.

26. Zaytsev, V. P.; Mertsalov, D. F.; Trunova, A. M.; Khanova, A. V.; Nikitina, E. V.; Sinelshchikova, A. A.; Grigoriev, M. S. Iodine Acetate as a Mild Selective Agent for the Wagner – Meerwein Rearrangement in 3a,6-Epoxyisoindoles *Chemistry of Heterocyclic Compounds*. **2020**, *56(7)*, 930 – 935.

27. Scholl, M.; Ding, S.; Lee, C. W.; Grubbs, R. H. Synthesis and Activity of a New Generation of Ruthenium-Based Olefin Metathesis Catalysts Coordinated with 1,3-Dimesityl-4,5-dihydroimidazol-2-ylidene Ligands *Org. Lett.* **1999**, *1*, 953 – 956.

28. Choi, T. L.; Lee, C. W.; Chatterjee, A. K.; Grubbs, R. H. Olefin Metathesis Involving Ruthenium Enoic Carbene Complexes *J. Am. Chem. Soc.* **2001**, *123*, 10417-10418.

29. Pal, S.; Alizadeh, M.; Kilbinger, A. F. M. Telechelics Based on Catalytic Alternating Ring-Opening Metathesis Polymerization *ACS Macro Lett.* **2019**, *8*, 1396-1401.

30. Sanford, M. S.; Ulman, M.; Grubbs, R. H. New Insights into the Mechanism of Ruthenium-Catalyzed Olefin Metathesis Reactions *J. Am. Chem. Soc.* **2001**, 123, 749 – 750.

31. Sanford, M. S.; Love, J. A.; Grubbs, R. H. Mechanism and Activity of Ruthenium Olefin Metathesis Catalysts *J. Am. Chem. Soc.* **2001**, *123*, 6543-6554.

32. Bielawski, C. W.; Grubbs, R. H. Highly efficient ring-opening metathesis polymerization (ROMP) using new ruthenium catalysts containing N-heterocyclic carbene ligands *Angew. Chem. Int. Ed.* **2000,** *39*, 2903 – 2906.

33. Bielawski, C. W.; Benitez, D.; Grubbs, R. H. Synthesis of end-functionalized poly (norbornene) s via ring-opening metathesis polymerization *Macromolecules*. **2001**, *34*, 8610 – 8618.

34. Scherman, O. A.; Kim, H. M.; Grubbs, R. H. Synthesis of Well-Defined Poly ((vinyl alcohol)2-alt-methylene) via Ring-Opening Metathesis Polymerization *Macromolecules*. **2002**, *35*, 5366 - 5371.

35. Choi, T. L.; Grubbs, R. H. Controlled Living Ring-Opening-Metathesis Polymerization by a Fast-Initiating Ruthenium Catalyst *Angew. Chem. Int. Ed.* **2003**, *42*, 1743 – 1746.

36. Yasir, M.; Liu, P.; Markwart, J. C.; Suraeva, O.; Wurm, F. R.; Smart, J.; Lattuada, M. and Kilbinger, A. F. M. One-Step Ring Opening Metathesis Block-Like Copolymers and their Compositional Analysis by a Novel Retardation Technique *Angew. Chem. Int. Ed.* **2020**, *59*, 13597 –13601.

graphical abstract